J|A|C|S
ARTICLES

Published on Web 08/09/2008

# Chiral Kagomé Lattice from Simple Ditopic Molecular Bricks

U. Schlickum,[*,#] R. Decker,[#] F. Klappenberger,[#,†] G. Zoppellaro,[‡] S. Klyatskaya,[‡] W. Auwärter,[#,†] S. Neppl,[†] K. Kern,[#,§] H. Brune,[#] M. Ruben,[*,‡] and J. V. Barth[*,#,†,⊥]

*Institut de Physique des Nanostructures, Ecole Polytechnique Fédérale de Lausanne, CH-1015 Lausanne, Switzerland, Physik Department E20, Technische Universität München, D-85748 Garching, Germany, Institut für Nanotechnologie, Forschungszentrum Karlsruhe, D-76021 Karlsruhe, Germany, Max-Planck-Institut für Festkörperforschung, D-70569 Stuttgart, Germany, and PHAS-AMPEL, University of British Columbia, Vancouver V6T 1Z4, Canada*

Received April 16, 2008; E-mail: uta.schlickum@epfl.ch; Mario.Ruben@int.fzk.de; jvb@ph.tum.de

***Abstract:*** Self-assembly techniques allow for the fabrication of highly organized architectures with atomic-level precision. Here, we report on molecular-level scanning tunneling microscopy observations demonstrating the supramolecular engineering of complex, regular, and long-range ordered periodic networks on a surface atomic lattice using simple linear molecular bricks. The length variation of the employed *de novo* synthesized linear dicarbonitrile polyphenyl molecules translates to distinct changes of the bonding motifs that lead to hierarchic order phenomena and unexpected changes of the surface tessellations. The achieved 2D organic networks range from a close-packed chevron pattern via a rhombic network to a hitherto unobserved supramolecular chiral kagomé lattice.

## Introduction

The spontaneous formation of regular patterns is among the most intriguing expressions in nature.[1] Notably, biologically inspired self-assembly provides pathways to achieve an amazing variety of supramolecular nanostructures and highly organized networks.[2,3] In recent years, self-assembly of organic species at crystalline surfaces has attracted widespread interest, and with the design of functional molecular building blocks, a great variety of surface architectures could be fabricated,[4−6] frequently showing unique chiral features.[7−9] The control of structures that display hierarchical order represents a current challenge,[6] albeit promising results could be demonstrated for several surface self-assembly systems.[10] Very recently, also the expression of coexisting nonperiodic and periodic arrangements (distorted pentagons, hexagons, and heptagons) from conformationally flexible rubrene molecules on the Au(111) surface was reported.[11] However, the realization of regular complex (chiral) topologies and surface tessellations remains largely unexplored, although they are frequently associated with particularly interesting physical and chemical properties.[3,12−14] Surface tessellations are similarly interesting from a mathematical point of view, where Johannes Kepler recognized already that, in the

# Ecole Polytechnique Fédérale de Lausanne.
† Technische Universität München.
‡ Forschungszentrum Karlsruhe.
§ Max-Planck-Institut für Festkörperforschung.
⊥ University of British Columbia.

(1) Ball, P. *The Self-Made Tapestry: Pattern Formation in Nature*; Oxford University Press: New York, 1999.
(2) Lehn, J.-M. *Supramolecular Chemistry, Concepts and Perspectives*; VCH: Weinheim, 1995; Vol. 227. Lawrence, D. S.; Jiang, T.; Levett, M. *Chem. Rev.* **1995**, *95*, 2229–2260. Philp, D.; Stoddart, J. F. *Angew. Chem., Int. Ed.* **1996**, *35*, 1154–1196.
(3) Moulton, B.; Zaworotko, M. J. *Chem. Rev.* **2001**, *101*, 1629–1658.
(4) Böhringer, M.; Morgenstern, K.; Schneider, W.-D.; Berndt, R.; Mauri, F.; Vita, A. D.; Car, R. *Phys. Rev. Lett.* **1999**, *83*, 324–327. Barth, J. V.; Weckesser, J.; Cai, C.; Günter, P.; Bürgi, L.; Jeandupeux, O.; Kern, K. *Angew. Chem., Int. Ed.* **2000**, *39*, 1230–1234. Otero, R.; Schöck, M.; Molina, L. M.; Laegsgaard, E.; Stensgaard, I.; Hammer, B.; Besenbacher, F. *Angew. Chem., Int. Ed.* **2004**, *44*, 2–6. Theobald, J. A.; Oxtoby, N. S.; Phillips, M. A.; Champness, N. R.; Beton, P. H. *Nature* **2003**, *424*, 1029–1031. De Feyter, S.; De Schryver, F. C. *Chem. Soc. Rev.* **2003**, *32*, 139–150. Barth, J. V.; Costantini, G.; Kern, K. *Nature* **2005**, *437*, 671–679. Cañas-Ventura, M. E.; Xiao, W.; Wasserfallen, D.; Müllen, K.; Brune, H.; Barth, J. V.; Fasel, R. *Angew. Chem., Int. Ed.* **2007**, *46*, 1814–1818.
(5) Yokoyama, T.; Yokoyama, S.; Kamikado, T.; Okuno, Y.; Mashiko, S. *Nature* **2001**, *413*, 619–621.
(6) Barth, J. V. *Annu. Rev. Phys. Chem.* **2007**, *58*, 375–407.
(7) Kühnle, A.; Linderoth, T. R.; Hammer, B.; Besenbacher, F. *Nature* **2002**, *415*, 891–893. Barlow, S. M.; Raval, R. *Surf. Sci. Rep.* **2003**, *50*, 201–341. Chen, Q.; Richardson, N. V. *Nat. Mater.* **2003**, *2*, 324–328. Vidal, F.; Delvigne, E.; Stepanow, S.; Lin, N.; Barth, J. V.; Kern, K. *J. Am. Chem. Soc.* **2005**, *127*, 10101–10106. Ernst, K. H. *Top. Curr. Chem.* **2006**, *265*, 209–252. Dmitriev, A.; Seitsonen, A. P.; Spillmann, H.; Lin, N.; Strunskus, T.; Wöll, C.; Barth, J. V.; Kern, K. *ChemPhysChem* **2006**, *7*, 2197–2204. Schiffrin, A.; Riemann, A.; Auwärter, W.; Pennec, Y.; Weber-Bargioni, A.; Cvetko, D.; Cossaro, A.; Morgante, A.; Barth, J. V. *Proc. Natl. Acad. Sci. U.S.A.* **2007**, *104*, 5279.
(8) Barth, J. V.; Weckesser, J.; Trimarchi, G.; Vladimirova, M.; Vita, A. D.; Cai, C.; Brune, H.; Günter, P.; Kern, K. *J. Am. Chem. Soc.* **2002**, *124*, 7991–8000.
(9) Fasel, R.; Parschau, M.; Ernst, K. H. *Nature* **2006**, *439*, 449–452.
(10) Spillmann, H.; Dmitriev, A.; Lin, N.; Messina, P.; Barth, J. V.; Kern, K. *J. Am. Chem. Soc.* **2003**, *125*, 10725–10728. Blüm, M.-C.; Cavar, E.; Pivetta, M.; Patthey, F.; Schneider, W.-D. *Angew. Chem., Int. Ed.* **2005**, *44*, 5334–5337. Clair, S.; Pons, S.; Brune, H.; Kern, K.; Barth, J. V. *Angew. Chem., Int. Ed.* **2005**, *44*, 7294. van Hameren, R.; Schön, P.; van Buul, A. M.; Hoogboom, J.; Lazarenko, S. V.; Gerritsen, J. W.; Engelkamp, H.; Christianen, P. C. M.; Heus, H. A.; Maan, J. C.; Rasing, T.; Speller, S.; Rowan, A. E.; Elemans, J. A. A. W.; Nolte, R. J. M. *Science* **2006**, *314*, 1433. Staniec, P. A.; Perdigao, L. M. A.; Saywell, A.; Champness, N. R.; Beton, P. H. *ChemPhysChem* **2008**, *8*, 2177.
(11) Pivetta, M.; Blüm, M.-C.; Patthey, F.; Schneider, W.-D. *Angew. Chem., Int. Ed.* **2008**, *47*, 1076.

 **10.1021/ja8028119 CCC: $40.75** 

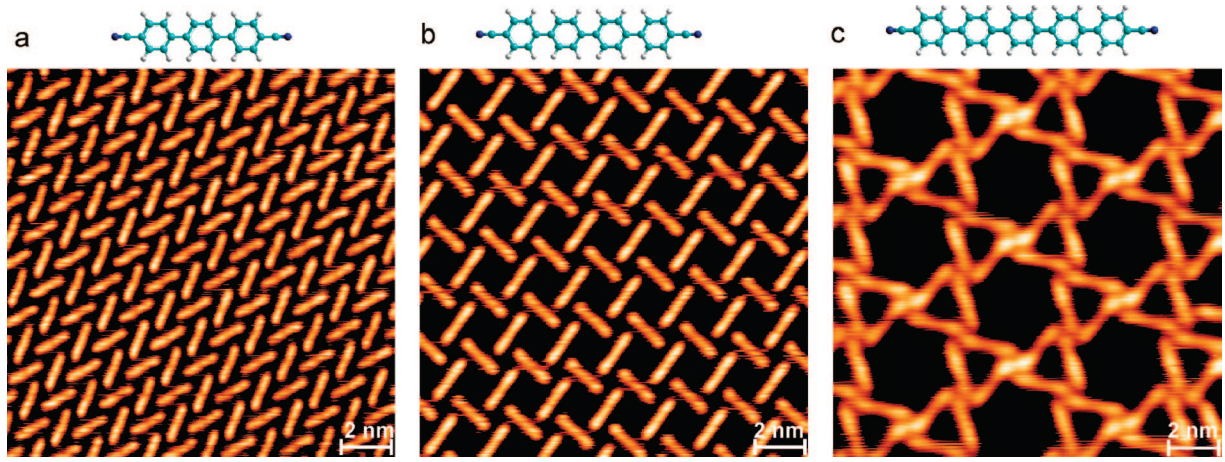


***Figure 1.*** Steering network complexity with the extension of the molecules self-assembled on the Ag(111) surface. (a) Densely packed chevron layer formed by the NC-$Ph_3$-CN species. (b) NC-$Ph_4$-CN molecules assemble in an open rhombic network. (c) Kagomé lattice formed by NC-$Ph_5$-CN molecules, comprising four-fold nodes and quasi-hexagonal and trigonal cavities. These images and the following were taken at surfaces covered with the molecular networks in the submonolayer regime and were recorded at 10 K. Structure models of molecular building blocks are depicted above the STM images. Their respective lengths are 1.66, 2.09, and 2.53 nm (light blue, C; dark blue, N; gray, H).

Euclidean plane, only 11 tessellations based on symmetric polygons are generally possible.[15] In particular, the semiregular trihexagonal uniform tiling where two triangles and two hexagons join at each vertex is also known in natural sciences as "kagomé" lattice.[16]

Here we present a systematic self-assembly study using linear dicarbonitrile−polyphenyl species on a Ag(111) surface. Our scanning tunneling microscopy (STM) observations show regular organic networks with increasing complexity upon extending the length of the employed simple ditopic molecular bricks. The series reflects distinct surface tessellations and is culminating in a hitherto unobserved nanoporous 2D chiral kagomé lattice composed of a topologically hierarchical structure. The observed complex tiling schemes represent novel variants related to the classic Archimedean (uniform) tessellations of the Euclidean plane.

## Results and Discussion

For our investigations, we synthesized a series of simple linear ditopic dicarbonitrile−polyphenyl molecules, NC-$Ph_n$-CN (Figure 1 insets), the lengths of which are varied from 1.7 to 2.5 nm (N···N distances) by the number of phenyl groups incorporated ($n = 3, 4, 5$). To design the NC-$Ph_4$-CN and NC-$Ph_5$-CN rod-like molecules, a new synthesis was developed, based on Suzuki coupling schemes (see Supporting Information). The reactivity of the carbonitrile endgroup has been successfully employed for 2D supramolecular engineering using meso-substituted porphyrin molecules.[5,17] The molecular-level STM data reproduced in Figure 1, recorded at 10 K, show a series of 2D supramolecular networks formed upon the deposition of the molecular building blocks on atomically flat and clean Ag(111) terraces at a substrate temperature of 300 K. Individual NC-$Ph_n$-CN molecules are resolved as rod-like protrusions. The monolayer height, single-phase organic networks form domains extending over square-micrometer large areas. The STM topographs show parts of larger network domains where a varying degree of network complexity is apparent, depending on the length of the employed molecules. While the NC-$Ph_3$-CN species form a densely packed chevron pattern (Figure 1a), the addition of one further phenyl group in the molecular backbone triggers a spreading into an open geometry comprising rhombic cavities and a distinct four-fold nodal coupling motif (Figure 1b).

The network topology becomes even more complex with the dicarbonitrile−pentaphenyl NC-$Ph_5$-CN building blocks that assemble in an intricate nanoporous lattice where the hexagonal substrate symmetry is retrieved. A closer inspection of the corresponding STM image in Figure 1c reveals that this network comprises the distinct features of a 2D kagomé lattice; i.e., it is composed of interlaced triangular units enclosing quasi-hexagonal nanocavities, the nodes of which connect the end-groups of four neighboring molecules.[13,16] The lattice represents a topologically hierarchical structure composed of simple linear bricks that are arranged in triangular subunits that again assemble around a hexagonal spacing. Thus, we are dealing with a geometry organized at multiple levels: linear bricks → open triangles → nanoporous kagomé lattice.

To obtain a deeper insight into the supramolecular ordering, we recorded high-resolution STM topographs. The observed packing of the NC-$Ph_3$-CN chevron layer depicted in Figure 2a can be interpreted in terms of the space-filling principle, repulsive N···N interactions, and the attractive interaction between the carbonitrile groups and the H-atoms of the phenyl rings (see ref 17). The latter is schematically shown in the model in Figure 2b. A closer inspection of the network reveals that, within one domain, the molecules lie along only two directions. These two orientations appear with different apparent heights in the STM images. The situation becomes more complicated when analyzing the pattern of the organic network formed by the NC-$Ph_4$-CN molecules (Figure 2c,d). We find extended domains with opposite chirality. As the molecular building blocks themselves are achiral, the chirality is caused by the polar nature of the CN endgroups, preventing a straight orientation toward the node center.[17] This renders a symmetric structure impossible and leads to a clockwise or anticlockwise rotational arrangement within the node for these highly symmetric building

(12) Newkome, G. R.; Wang, P.; Moorefield, C. N.; Cho, T. J.; Mohapatra, P. P.; Li, S.; Hwang, S.-H.; Lukoyanova, O.; Echegoyen, L.; Palagallo, J. A.; Iancu, V.; Hla, S.-W. *Science* **2006**, *312*, 1782–1785.
(13) Ramirez, A. P. *Annu. Rev. Mater. Sci.* **1994**, *1994*, 453–480.
(14) Elser, V. *Phys. Rev. Lett.* **1989**, *62*, 2405–2408.
(15) Kepler, J. *Harmonice Mundi*; 1619. Grünbaum, B.; Shephard, G. C. *Tilings and Patterns*; W.H. Freeman: New York, 1987.
(16) Syôzi, I. *Prog. Theor. Phys.* **1951**, *6*, 306–308.
(17) Okuno, Y.; Yokoyama, T.; Yokoyama, S.; Kamikado, T.; Mashiko, S. *J. Am. Chem. Soc.* **2002**, *124*, 7218–7225.

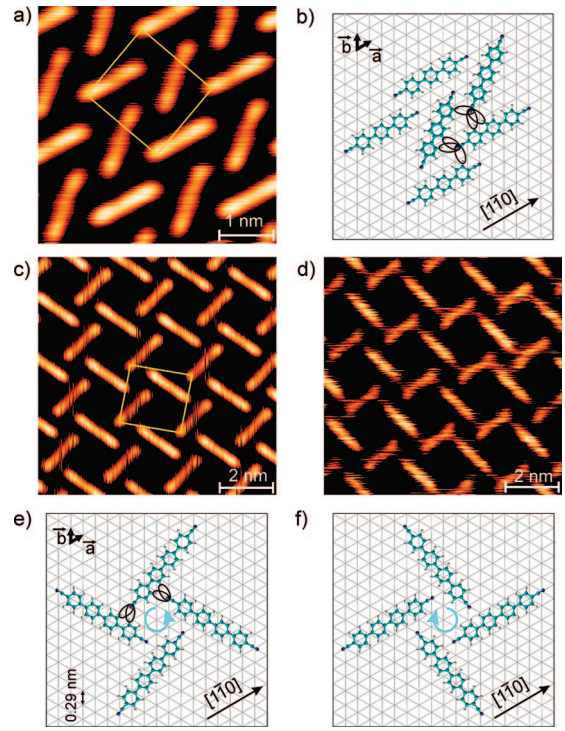


***Figure 2.*** (a) High-resolution STM image showing the molecular packing in the NC-$Ph_3$-CN chevron layer mediated by the carbonitrile endgroups. (b) Corresponding model showing the interaction between adjacent carbonitrile and phenyl groups. (c,d) Nanoporous lattices with opposite chirality realized with the NC-$Ph_4$-CN molecules. The chirality is stressed in the model showing common 2D chiral rotor motifs (e,f). The intersection points of the underlying grid in the models (b,e,f) represent the atomic positions of the Ag(111) surface. The rectangles in (a) and (c) indicate the unit cells of the systems.

blocks. The elementary 2D rotor motifs are shown in Figure 2e,f, which also illustrates how the four molecules are connected within the node. The almost perpendicular arrangement of the molecules in the rotor motif indicates a modified lateral bonding scheme compared to the NC-$Ph_3$-CN species. Also for the rhombic network, molecules align in only two directions within a given domain. Again, the different orienations are imaged with different apparent heights.

Notably, the absence of moiré patterns larger than the unit cell of the organic networks shows that all superstructures are commensurate with respect to the underlying atomic lattice.[8,18] On the basis of the topography and assuming the same size of the molecules as in the gas phase with a planar arrangement at the surface, we obtain average lengths of about 0.33 ± 0.03 and 0.27 ± 0.04 nm for the H···N bonds of NC-$Ph_3$-CN and NC-$Ph_4$-CN networks, respectively, in agreement with earlier reports.[5,17,19] The models in Figure 2b,e,f are based on the average of H···N bond lengths for each of the individual bonds indicated in Figure 2b,e and the averaged angle between adjacent molecules determined by several large-scale STM images. We found that, for the rhombic network formed by NC-$Ph_4$-CN molecules and the chevron pattern assembled by NC-$Ph_3$-CN, only one configuration is possible where, within the error bars, all N-atoms lie on identical sites on the subjacent Ag(111) lattice. In these arrangements, both molecular networks are commensurate with the underlying Ag(111) surface, and in both patterns, half of the molecules lie along the [1 $\bar{1}$ 0] direction, while the other half lie along [7 $\bar{3}$ $\bar{4}$] and [3 5 $\bar{8}$] for NC-$Ph_3$-CN and NC-$Ph_4$-CN, respectively. The preferred ⟨1 $\bar{1}$ 0⟩ orientation for polyphenyl molecular backbones is supported by the observation that, e.g., single sexiphenyl molecules and, in the submonolayer coverage, quaterphenyl molecules with a weak intermolecular interaction self-assemble along this high-symmetry axis on Ag(111) and Au(111) surfaces, respectively.[20] The indicated unit cells of the networks are given by

$$\begin{pmatrix} 4 & 2 \\ -5 & 6 \end{pmatrix}\begin{pmatrix} \vec{a} \\ \vec{b} \end{pmatrix} \quad \text{and} \quad \begin{pmatrix} 1 & 7 \\ 9 & -5 \end{pmatrix}\begin{pmatrix} \vec{a} \\ \vec{b} \end{pmatrix}$$

for Figure 2a and c respectively, with $\vec{a}$ and $\vec{b}$ being the Ag(111) unit vectors.

Under the conservation of the H···N bond lengths and angles between adjacent molecules, the NC-$Ph_3$-CN and NC-$Ph_5$-CN molecules cannot be arranged in a commensurate rhombic network like that formed by NC-$Ph_4$-CN. Furthermore, it is impossible for NC-$Ph_4$-CN and NC-$Ph_5$-CN molecules to form the chevron pattern of NC-$Ph_3$-CN since an increase in the molecular length leads automatically to a widening of the structure and thus to increased H···N bond lengths. Therefore, our model suggests that one driving force for the different organic architectures is the interplay between intermolecular interactions and the epitaxial fit to the Ag atomic lattice.[8,18]

In the STM images (cf. Figure 2a,c), the observed highly regular pattern of different brightness supports our model and thus the arguments of the commensurate networks. Molecules aligned along two different crystallographic directions likely have different molecular substrate interactions and hence different electronic structures.

The most complex structure occurs for the NC-$Ph_5$-CN molecules. An overview image and high-resolution data of the resulting networks are presented in Figure 3, along with a model for the kagomé lattices. A detailed inspection of the nodal structure resolved in the STM images reveals that, with the present system, a novel variant of a trihexagonal tiling scheme is encountered, namely a 2D chiral kagomé lattice (Figure 3c,d). As in the case of the NC-$Ph_4$-CN molecules, the chirality is introduced by the polar nature of CN endgroups interacting with aromatic rings. Accordingly, the enantiomorphic kagomé lattice is composed of chiral triangular subunits formed by the linear molecules that are slightly rotated from the kagomé symmetry axes (see schematic drawing in Figure 3e,f). This hierarchical and nanoporous assembly contrasts the coupling schemes of compounds forming kagomé lattices reported to date: layered oxides,[13] dehydrogenation of diaminoperylene−quinone−diimine,[21] jarosites,[22] or metal−organic networks,[23] where the incorporated metal centers account for both the ordering and the intriguing magnetic properties of the material. [13,16,22,23] Further examples of kagomé networks reported in the literature include $^3$He layers[14] and alkyl-substituted dehydrobenzol-annulene compounds[24] on graphite, as well as engineered DNA

(18) Auwärter, W.; Weber-Bargioni, A.; Schiffrin, A.; Riemann, A.; Fasel, R.; Gröning, O.; Barth, J. V. *J. Chem. Phys.* **2006**, *124*, 194708.
(19) Li, Y.; Li, F.; Zhang, X.; Xie, Z.; Xie, W.; Xu, H.; Li, B.; Shen, F.; Hanif, M.; Ma, D.; Ma, Y. *Chem. Commun.* **2007**, 231–233.
(20) Braun, K.-F.; Hla, S.-W. *Nano Lett.* **2005**, *5*, 73–76. Müllegger, S.; Salzmann, I.; Resel, R.; Hlawacek, G.; Teichert, C.; Winkler, A. *J. Chem. Phys.* **2004**, *121*, 2272.
(21) Stöhr, M.; Wahl, M.; Spillmann, H.; Gade, L. H.; Jung, T. A. *Small* **2007**, *3*, 1336.
(22) Grohol, D.; Matan, K.; Cho, J.-H.; Lee, S.-H.; Lynn, J. W.; Grocera, D. G.; Lee, Y. S. *Nat. Mater.* **2005**, *4*, 323–328.
(23) Moulton, B.; Lu, J.; Hajndl, R.; Hariharan, S.; Zaworotko, M. J. *Angew. Chem., Int. Ed.* **2002**, *41*, 2821–2824.

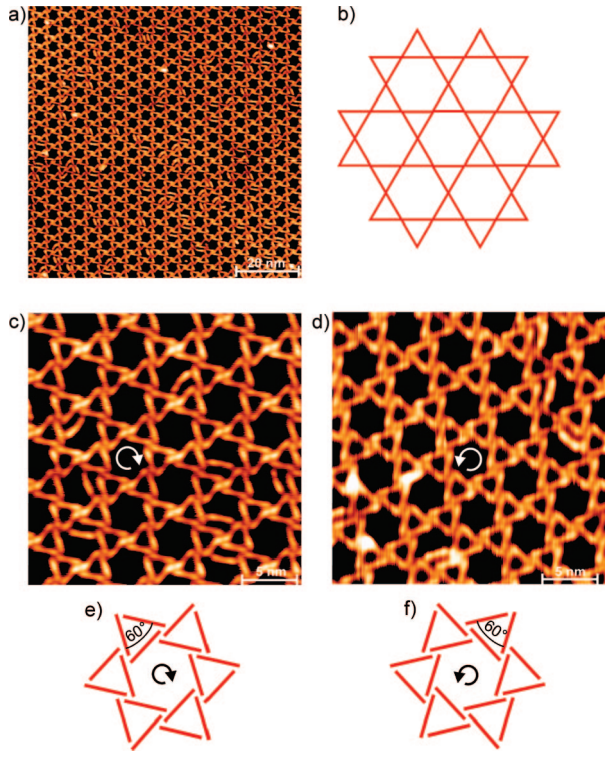


***Figure 3.*** Kagomé lattice and the two mirror-symmetric representations for NC-$Ph_5$-CN networks. (a) Large-scale STM topograph showing the long-range order of the supramolecular network. (b) The classical kagomé lattice is defined by interlaced triangles where each node has four neighboring nodes. (c,d) The arrangement of the NC-$Ph_5$-CN molecules defines a 2D chiral variant of the kagomé lattice; clockwise and anticlockwise rotation direction is indicated by the arrows. The inner diameter of the enclosed quasi-hexagonal cavities is approximately 4 nm. (e,f) Schematic drawing of the kagomé lattices with opposite chirality.

crystals.[25] In contrast to the recent report of a related structure of solution-deposited tetraacids on a graphitic substrate, where a kagomé arrangement is programmed by the tecton's functionalities,[26] the present kagomé ordering is truly obtained by supramolecular self-assembly from simple, low-symmetric linear molecules. It extends over large areas as single domains, whereby the few lattice defects consist almost exclusively of an additional molecule caught within a hexagonal cavity. Only for coverages close to one monolayer, the structure is transformed into a densely packed pattern because of steric constraints (see Supporting Information).

The nodal structure of the NC-$Ph_5$-CN kagomé lattice is different from the chiral rotor motif and the chevron pattern realized with the NC-$Ph_4$-CN and NC-$Ph_3$-CN species (cf. Figure 2). The molecular endgroups in the kagomé networks come much closer than in the topologically simpler lattices discussed above; i.e., in the STM data they seem to touch each other, while they are clearly separated by a topographic gap for the other systems described. If we assume that the molecules are adsorbed in a strictly planar conformation, we find an unrealistically small H···N distance of about 0.15 ± 0.03 nm.

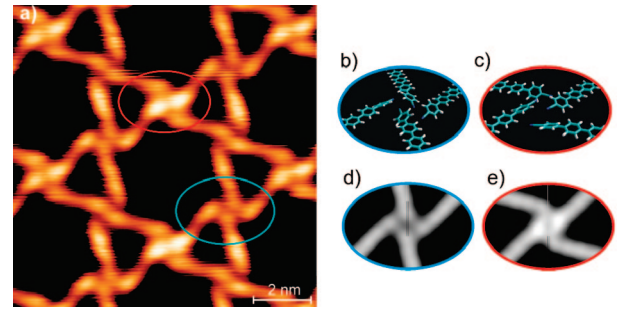


***Figure 4.*** The nodal structure of the 2D chiral kagomé lattice is associated with a nonplanar adsorption geometry of the CN-$Ph_5$-CN building blocks. (a) High-resolution STM image identifying the two different types of nodes in the kagomé lattice. (b,c) 3D representations of structural models of two specific nonplanar nodal geometries associated with molecular flexure. (d,e) The corresponding charge density contour plots mimic the main features of the experimental data.

Thus, flat bonding must be excluded in view of the interaction potentials. In addition, we again observe differences in the imaged brightness within the network architecture. Always two opposite-facing nodes of a hexagon appear brighter and four darker.

To evaluate the assumption that the NC-$Ph_5$-CN molecules are not adsorbed onto the Ag(111) surface in a flat configuration, we performed near-edge X-ray absorption fine-structure spectroscopy (NEXAFS) measurements, which allows determining the geometrical alignment of molecular units on surfaces.[27,28] A comparative study of the NC-$Ph_3$-CN phase and the NC-$Ph_5$-CN kagomé phase (see Supporting Information) reveals that the terminal benzonitrile group of the NC-$Ph_3$-CN molecules adopts a strictly flat alignment on the surface, whereas that of the NC-$Ph_5$-CN molecules shows a significant rotation (approximately 20°) around the long molecular axis.

To obtain a better understanding of the node structure itself, we modeled the kagomé lattice nodes with a simple procedure employing different configurations of 2D confined molecules in the framework of the extended Hückel theory (see Experimental Section). Notably, we allowed the conformational adaptation of the inner moieties, while the relative positions of the four molecules forming one node were fixed, in full compliance with the STM data. This geometry optimization yields nodal structures characterized by a rotation of the terminal Ph-CN groups around the $\sigma$-bond axis and molecular flexure implying a bending of the polyphenyl backbone. To further analyze the experimental findings, we mimicked STM images of the kagomé lattice nodes, focusing on two specific, highly symmetric nodal geometries exhibiting the lowest total energies (Figure 4b,c) and compared them to a typical experimental image (Figure 4a). The two underlying geometries differ in the relative orientation of the NC-Ph endgroups: while the nodal structure displayed in Figure 4b is characterized by a propeller-like arrangement of the terminal moieties, Figure 4c represents two pairs of inner groups alternatingly tilted out of the surface

(24) Furukawa, S.; Uji-i, H.; Tahara, K.; Ichikawa, T.; Sonoda, M.; De Schryver, F. C.; Tobe, Y.; De Feyter, S. *J. Am. Chem. Soc.* **2006**, *128*, 3502–3503.
(25) Malo, J.; Mitchell, J. C.; Vénien-Dryan, C.; Harris, J. R.; Wille, H.; Sherratt, D. J.; Turberfield, A. J. *Angew. Chem., Int. Ed.* **2005**, *44*, 3057–3061.
(26) Zhou, H.; Dang, H.; Yi, J. H.; Nanci, A.; Rochefort, A.; Wuest, J. D. *J. Am. Chem. Soc.* **2007**, *129*, 13774.
(27) Stöhr, J. *NEXAFS Spectroscopy*; Springer: Heidelberg, Germany, 1991.
(28) Klappenberger, F.; Cañas-Ventura; M. E.; Clair, S.; Pons, S.; Schlickum, U.; Kern, K.; Brune, H.; Qiu, Z.-R.; Ruben, M.; Strunskus, T.; Wöll, C.; Comisso, A.; Vita, A. D.; Barth, J. V. *ChemPhysChem* **2007**, *8*, 1782–1786. Auwärter, W.; Klappenberger, F.; Weber-Bargioni, A.; Schiffrin, A.; Strunskus, T.; Wöll, C.; Pennec, Y.; Riemann, A.; Barth, J. V. *J. Am. Chem. Soc.* **2007**, *129*, 11279. Weber-Bargioni, A.; Auwärter, W.; Klappenberger, F.; Reichert, J.; Lefrançois, S.; Strunskus, T.; Wöll, C.; Schiffrin, A.; Pennec, Y.; Barth, J. V. *ChemPhysChem* **2008**, *9*, 89–94.

plane. Both contour plots mimic the essential features within the kagomé nodes. While our calculations consider only an isolated four-molecule node system and do not directly include the underlying surface, the latter presumably plays a role beyond simply supporting the kagomé lattice. Likely the different node configurations and their long-range order are induced by the stacking with respect to the Ag lattice.

It is also interesting to note that a related four-fold coupling motif of carbonitrile units has been identified in crystallized lanthanide complexes[29] that reflects an attractive interaction between CN groups and the phenyl $\pi$-system.[30] This suggests that the terminal Ph-CN groups of the NC-$Ph_5$-CN species are rotated to form a CN $\pi$-bond instead of the CN−H linkage that is reflected in the packing scheme of the shorter molecules. The net result of the modeling and the NEXAFS data hence corroborates the indications from the NC-$Ph_5$-CN linkers' STM appearance and emphasizes the importance of conformational adaptation in 2D supramolecular engineering.[28] Thus, it is obvious that the energy landscapes driving the ultimate structure formation in 2D self-assembly phenomena undergo surprising changes, depending on the molecular length. From the supramolecular engineering point of view, aiming at the design of molecular building blocks to program a certain structural outcome, this calls for an improved theoretical description of noncovalent synthesis using adsorbed species.

Finally, it is worth mentioning that subsequent deposition of Co-atoms onto the organic structures leads to metal−ligand interactions between the provided Co centers and the carbonitrile endgroups. As a result, the variety of bonding motifs in the organic layers—chevron pattern, rhombic network, and kagomé lattice—is reduced to a unique three-fold coordination of Co centers.[31] This leads to mesoscopically well-ordered honeycomb nanomeshes, providing open pores, the size of which is tuned by the length of the employed molecular bricks.[32]

## Conclusion

In conclusion, our findings show that highly organized supramolecular chiral networks with multilevel order can be realized by self-assembly protocols employing simple ditopic molecular bricks at the hexagonal Ag(111) surface. The observed patterns are directly related to classical theories from geometry dealing with the uniform tiling of planes.[15] Their complexity increases with the constituents' length, whereas the different architectures are associated with the interplay between substrate epitaxial fit, noncovalent lateral interactions, and the molecules' conformational flexibility. It is particularly fascinating that a linear molecular building block suffices to fabricate a new variant of a trihexagonal uniform tiling, i.e., a 2D chiral kagomé lattice. The topologically hierarchical structure of this complex, enantiomorphic superlattice reflects a distinct conformational adaptation of the molecular endgroups. It is thus suggested that unique bonding motifs and supramolecular surface patterns can be achieved with adsorbed flexible molecular units; i.e., surface-confined self-assembly protocols using tailored adaptive molecular species open the way to engineer complex hierarchic nanoarchitectures, which set the base for further functionalization.

## Experimental Section

The STM measurements were performed under ultrahigh vacuum ($1 \times 10^{-10}$ mbar) in a chamber equipped with standard tools for surface preparation and characterization. We used a home-built low-temperature STM operating at $T \approx 10$ K.[33] For the self-assembly, the molecules were vapor-deposited from a Knudsen cell evaporator heated to 460, 490, and 535 K for NC-$Ph_3$-CN, NC-$Ph_4$-CN, and NC-$Ph_5$-CN, respectively. The Ag(111) surface was held at 300 K during the deposition. The experiments were typically carried out with a coverage of roughly 0.5 monolayer; however, the presented molecular architectures were found to be independent of the coverage as long as it is well below one monolayer. Typical STM imaging parameters were 0.1 nA and 0.5 V. We used a tungsten tip prepared by $Ar^+$ sputtering.

The molecule NC-$Ph_3$-CN was synthesized according a literature protocol.[34] Both compounds NC-$Ph_4$-CN and NC-$Ph_5$-CN were synthesized by a regular Suzuki coupling scheme involving the respective bis-iodophenylene precursors[35] and 4-phenylboronic acid in the presence of a catalytic amount of Pd(0). All compounds gave correct analytical data. Details on synthesis protocols are provided in the Supporting Information.

As a basis to corroborate and analyze the experimental structural data, we applied basic molecular mechanics calculations to optimize the geometry of the kagomé lattice nodes. Specifically, the MM+ force field of the Hyperchem 7.5 molecular modeling package was used to calculate and minimize the total energy of a four-molecule node. The STM image simulations are based on semiempirical extended Hückel calculations (HYPERCHEM, Hypercube Inc., Gainesville, FL). A constant electron density contour is obtained by integrating over the relevant molecular orbitals, which mimics a constant-current STM image. The STM data were recorded at a low positive sample bias voltage, thus representing the empty electronic states of the structure. Accordingly, the simulated STM images presented in Figure 4d,e are based on the density of states of the lowest unoccupied molecular orbitals (LUMO to LUMO+3) of the four-molecule system. The calculated charge density contour is blurred by a Gaussian filter to account for experimental broadening due to a finite tip radius. This procedure mimics the appearance of large molecules weakly adsorbed on surfaces.[9,18]

**Acknowledgment.** We thank A. Arnau and I. Silanes for stimulating discussions. We are grateful to Th. Strunskus and Ch. Wöll for support at the HE-SGM beamline at BESSY II. The code to mimic constant current STM images was kindly provided by O. Gröning and R. Fasel, EMPA Materials Science and Technology, Switzerland, 2004. This work was supported by the European Science Foundation Collaborative Research Programme FunSMARTs and by the DFG Cluster of Excellence Munich Center for Advanced Photonics. Traveling costs for synchrotron measurements were provided by the BMBF through grant no. 05ES3XBA/5.

**Supporting Information Available:** Extended description of the synthesis of compounds, additional figures, and discussion of near-edge X-ray absorption fine structure analysis. This material is available free of charge via the Internet at http://pubs.acs.org.

JA8028119

(29) Eliseeva, S. V.; Ryazanov, M.; Gumy, F.; Troyanov, S. I.; Lepev, L. S.; Bünzli, J.-C.; Kuzmina, N. P. *Eur. J. Inorg. Chem.* **2006**, 4809–4820.
(30) Tian, Z.; Ren, X.; Li, Y.; Song, Y.; Meng, Q. *Inorg. Chem.* **2007**, *46*, 8102.
(31) Stepanow, S.; Lin, N.; Payer, D.; Schlickum, U.; Klappenberger, F.; Zoppellaro, G.; Ruben, M.; Brune, H.; Barth, J. V.; Kern, K. *Angew. Chem., Int. Ed.* **2007**, *46*, 710–713.
(32) Schlickum, U.; Decker, R.; Klappenberger, F.; Zoppellaro, G.; Klyatskaya, S.; Ruben, M.; Silanes, I.; Arnau, A.; Kern, K.; Brune, H.; Barth, J. V. *Nano Lett.* **2007**, *7*, 3813–3818.
(33) Clair, S.; Pons, S.; Seitsonen, A. P.; Brune, H.; Kern, K.; Barth, J. V. *J. Phys. Chem. B* **2004**, *108*, 19392–19397.
(34) Collonge, J.; Buendia, J.; Sabadie, J. *Bull. Soc. Chem. Fr.* **1967**, 4370–4374.
(35) Merkushev, E. B.; Yudina, N. D. *Zh. Org. Khim.* **1981**, *17*, 2598–2601.